

Crystal Structure of a Four-Stranded Intercalated DNA:  $d(C_4)^{\dagger,\ddagger}$ 

Liqing Chen,\* Li Cai, Xiaohua Zhang, and Alexander Rich\*

Department of Biology, Massachusetts Institute of Technology, Cambridge, Massachusetts 02139

Received August 19, 1994; Revised Manuscript Received September 19, 1994<sup>®</sup>

**ABSTRACT:** The crystal structure of  $d(C_4)$  solved at 2.3-Å resolution reveals a four-stranded molecule composed of two interdigitated or intercalated duplexes. The duplexes are held together by hemiprotonated cytosine–cytosine base pairs and are parallel stranded, but the two duplexes point in opposite directions. The molecule has a slow right-handed twist of 12.4° between covalently linked cytosine base pairs, and the base stacking distance is 3.1 Å. This is in general agreement with the NMR studies. A biological role for DNA in this conformation is suggested.

One of the remarkable features of DNA is its structural polymorphism. We now know that beyond the DNA duplex it can also exist in a variety of other conformations involving either three strands or four and even in a left-handed form. Increasingly, we are coming to address the biology associated with different DNA conformations. Over 30 years ago it was discovered that the nucleic acid base cytosine could form a hydrogen-bonded pair with itself if it was hemiprotonated. This was first observed in the crystal of cytosine-5-acetic acid (Marsh et al., 1962). Shortly thereafter a fiber X-ray diffraction analysis of poly(cytidylic acid) (Langridge & Rich, 1963) was interpreted as indicating that two parallel strands were held together by this type of hydrogen bonding as the fiber was stabilized only when the pH was lowered below 7. A number of physical–chemical studies were carried out which made it clear that a pairing between cytosine and protonated cytosine  $C\cdot C^+$  (actually  $C\cdot CH^+$ ) was likely to be found in these structures (Akinrimisi et al., 1963; Hartman & Rich, 1965; Inman, 1964). About a year ago Gueron and his associates (Gehring et al., 1993) reported a four-stranded, intercalated structure for  $d(TC_5)$  based on the NMR spectrum. The structure is composed of two parallel-stranded duplexes with  $C\cdot C^+$  pairing which interpenetrate so that the base pairs from the two duplexes are interdigitated. Here we describe the X-ray crystallographic analysis of  $d(C_4)$ . This structure is in general agreement with the NMR studies and reveals many important features of the molecule.

## MATERIALS AND METHODS

The oligonucleotide  $d(C_4)$  was synthesized at the MIT Biopolymers Laboratory and purified by HPLC. The material was dissolved in solution to a concentration of 5.4 mM. Crystals were grown by vapor diffusion using the hanging drop method from a solution containing 2.7 mM  $d(C_4)$  and 100 mM sodium cacodylate buffer (pH 5.5) which was

equilibrated with a reservoir of 20% 2-methyl-2,4-pentanediol. Chunky crystals grew in the solution to a size of 0.3 mm after about a month. Data were collected on a Rigaku R-Axis II imaging plate to 2.3-Å resolution at room temperature. The crystal was quite robust, and there was very little decrement of diffraction intensity with time. An extensive search was carried out for heavy atom derivatives. Soaking with 1 mM  $K_2PtCl_6$  for 25 days yielded a crystal that showed significant differences in diffraction intensity without a change in the lattice constants. Heavy atom diffraction data were collected to 2.5-Å resolution. The isomorphous heavy atom difference Patterson revealed clear peaks with a minimum of background intensity. Likewise, the anomalous difference Patterson revealed the same set of peaks. A single site was identified on a 3-fold axis in the cubic lattice. The position of the platinum atom confirmed that the space group was  $I23$ . Phasing was carried out using single isomorphous replacement (SIR), as well as single-wavelength anomalous scattering (SAS) (Wang, 1985). In addition, solvent flattening was used to further refine the phases (Wang, 1985). The resultant electron density map clearly revealed the structure. The sugar phosphate backbones were clearly visible with intense peaks at the phosphate positions. In addition, individual bases were visible in the map. A model was built into the electron density map using the program FRODO (Jones, 1985). The initial  $R$ -factor was 44% for the data from 8 to 2.3 Å. Refinements were then carried out using the program X-PLOR (Brunger et al., 1989). Simulated annealing was used, and the  $R$ -factor rapidly fell to 23%. The original map was checked frequently during this refinement process.  $F_o - F_c$  maps were calculated, and residual density was assigned to water molecules for peaks  $3\sigma$  or greater. Several iterative cycles were carried out to identify more water molecules. The asymmetric unit contains 32 nucleotides, and 58 water molecules were identified in it as well. The statistics for the final refinement are shown in Table 1. The coordinates have been deposited in the Protein Data Bank.

## RESULTS

The molecule crystallizes in a cubic space group with eight strands in the asymmetric unit, a total of 32 nucleotides. The asymmetric unit consists of two quadruplexes which we label

<sup>†</sup> This research was supported by grants from the National Institutes of Health, the National Science Foundation, the Office of Naval Research, the American Cancer Society, the National Aeronautics and Space Administration, and the U.S. Department of Energy through the Los Alamos National Laboratory.

<sup>‡</sup> Coordinates have been deposited in the Brookhaven Protein Data Bank (Acquisition Number 190D).

\* Corresponding authors [telephone (617) 253-4715; FAX (617) 253-8699].

<sup>®</sup> Abstract published in *Advance ACS Abstracts*, November 1, 1994.

Table 1: Crystallographic Data

Table 1. Crystallographic Data

Space Group: Cubic $I23$ , $a = b = c = 82.3 \text{ \AA}$ , $\alpha = \beta = \gamma = 90^\circ$							
(a) Phasing Statistics: Pt Position $x = -0.194$ , $y = -0.194$ , $z = -0.194$							
derivative $K_2PtCl_6$	resolution ( $\text{\AA}$ )	reflection pairs	completeness (%)	$R_{\text{diff}}^a$ (%)	phasing power	figure of merit	
SIR (isomorphous)	2.5	3110	94	17.6	1.94	0.28	
SAS (anomalous)	2.5	2297	69	5.1	2.69	0.39	
merged (SIR + SAS)	2.5	3198	96			0.47	
after solvent flattening						0.73	
(b) Refinement Statistics							
resolution ( $\text{\AA}$ )	no. of reflections ( $I > 0$ )	completeness (%)	no. of non-hydrogen atoms	no. of water molecules	RMS bond lengths ( $\text{\AA}$ )	RMS bond angles (deg)	$R$ -factor <sup>b</sup>
8–2.3	4051	98	584	58	0.012	3.6	0.188

<sup>a</sup>  $R_{\text{diff}} = \sum |F_{\text{native}} - F_{\text{derivative}}| / \sum F_{\text{native}}$  for isomorphous data.  $R_{\text{diff}} = \sum |F_+ - F_-| / \sum \langle F \rangle$  for anomalous data. <sup>b</sup>  $R = \sum |F_o - F_c| / \sum F_o$ .

<sup>a</sup>  $R_{\text{diff}} = \sum |F_{\text{native}} - F_{\text{derivative}}| / \sum F_{\text{native}}$  for isomorphous data.  $R_{\text{diff}} = \sum |F_+ - F_-| / \sum \langle F \rangle$  for anomalous data. <sup>b</sup>  $R = \sum |F_o - F_c| / \sum F_o$ .

A and B, each containing four strands held together in an intercalative manner. The two quadruplexes are very similar to each other but not identical. When they are superimposed, the root mean square deviation between the atomic positions is 0.54  $\text{\AA}$ . The general features of the molecule are shown in Figures 1 and 2. The four strands in the quadruplex molecule are arranged so that the backbones are assembled in two closely adjacent pairs. Thus, the molecule is flat and ribbon shaped with a very wide groove on two sides and very narrow grooves at its ends. Figure 1A shows a stereo diagram of the molecule viewed largely from the wide groove side. The nucleotides are numbered at their 5' ends, and they occur in two groups. In the parallel-stranded duplex colored purple, the 5' ends are at the bottom, the strand containing nucleotides 1–4 is held together by  $C^+C$  pairing to the strand with nucleotides numbering 5–8. At the top of the diagram are the 5' ends of the remaining two strands. Nucleotides 9–12 paired to the strand containing nucleotides 13–16. This is the same orientation of nucleotide chains as deduced by Gehring et al. (1993). Figure 1B shows the same view with electron density nets contoured in blue. Figure 1C is a van der Waals representation of the same view showing the manner in which the four chains form a rather compact structure.

A skeletal end view of the molecule is seen in the stereo diagram of Figure 2. The molecules twist slowly in a right-handed manner. Close inspection of Figure 2 reveals some variability in the twist of the molecule. The average twist in molecules A and B is  $12.4^\circ$  with a standard deviation of  $3.6^\circ$ . Thus, one cytosine base pair is on average twisted  $12.4^\circ$  relative to its covalent neighbor. The distance between the nearest base pairs is 3.1  $\text{\AA}$ . This distance is the same as that measured in the fiber X-ray diagram of poly(cytidylic acid) (Hartman & Rich, 1965). The quadruplex has a pitch near 180  $\text{\AA}$ , the distance for the ribbon to make a complete turn of  $360^\circ$ . The molecule also has two quasi-2-fold rotational symmetry axes perpendicular to the helical axis. Thus, the twist will bring it back into approximately the same position in 90  $\text{\AA}$ .

**Closely Packed Chains.** There is a remarkably close packing between the two sugar phosphate chains at the narrow end of the twisted ribbon. This is shown in a skeletal stereo diagram in Figure 3A. The zigzag of the sugar phosphate chain of one strand is neatly complemented by the zigzag shape of the adjacent antiparallel strand. There

is some conformational variability in the strands leading to differences in the phosphorus–phosphorus distance between the adjacent chains at the narrow end of the molecule. The shortest P–P distances between chains are near 5.4  $\text{\AA}$ . (The shortest intrachain distance is 6.0  $\text{\AA}$ .) The longest P–P distances between the closely packed chains are somewhat over 10  $\text{\AA}$ . The average distance is 7.8  $\text{\AA}$ . These distances are somewhat larger than the shortest distances of 4.9  $\text{\AA}$  reported for the NMR study (Gehring et al., 1993). The reason for this arises from small differences in the relative placement of the two chains and changes in torsional angles in the backbone seen in the crystal structure which tend to increase the interstrand P–P distances. The variability arises from the fact that the molecule appears to have considerable potential for flexible movement in the phosphate positions, even though the overall molecule appears to be quite regular.

The close fitting of the chains is also illustrated in the van der Waals diagrams of Figure 3, panels B and C. Figure 3B shows the two chains closest to the reader in the stereo diagram of Figure 3A. The variability in the conformations of the phosphate groups on adjacent chains can be readily seen. At the same time the relative closeness of the two chains is apparent. Figure 3C shows a van der Waals view of the two chains furthest away from the reader in Figure 3A. The cytosine residues are in front of this molecule, and the sugar phosphate chains lie behind it.

There is an interesting asymmetry in the narrow grooves at either end of the flat ribbon. The groove closer to the reader in Figure 3A is shown in Figure 3B. The average P–P distance across the groove is  $7.1 \pm 1.0 \text{ \AA}$ . However, in the two strands furthest from the reader in Figure 3A shown in Figure 3C, the average distance is  $8.4 \pm 1.6 \text{ \AA}$ . This asymmetry is found in both molecule A and molecule B. There seems to be a subtle influence in the molecule that prevents them from being completely symmetric. In the NMR time scale, the molecule is observed to have 2-fold symmetry in three different mutually perpendicular directions (Gehring et al., 1993). That symmetry is not maintained in the crystal structure. The average phosphorus–phosphorus distance across the wide groove is  $15.9 \pm 0.67 \text{ \AA}$ . There is no significant difference between the two sides of the molecule.

One of the predominant NMR signals that characterizes the intercalative quadruplex is the interaction between the H1' protons of two different adjacent chains (Gehring et al.,



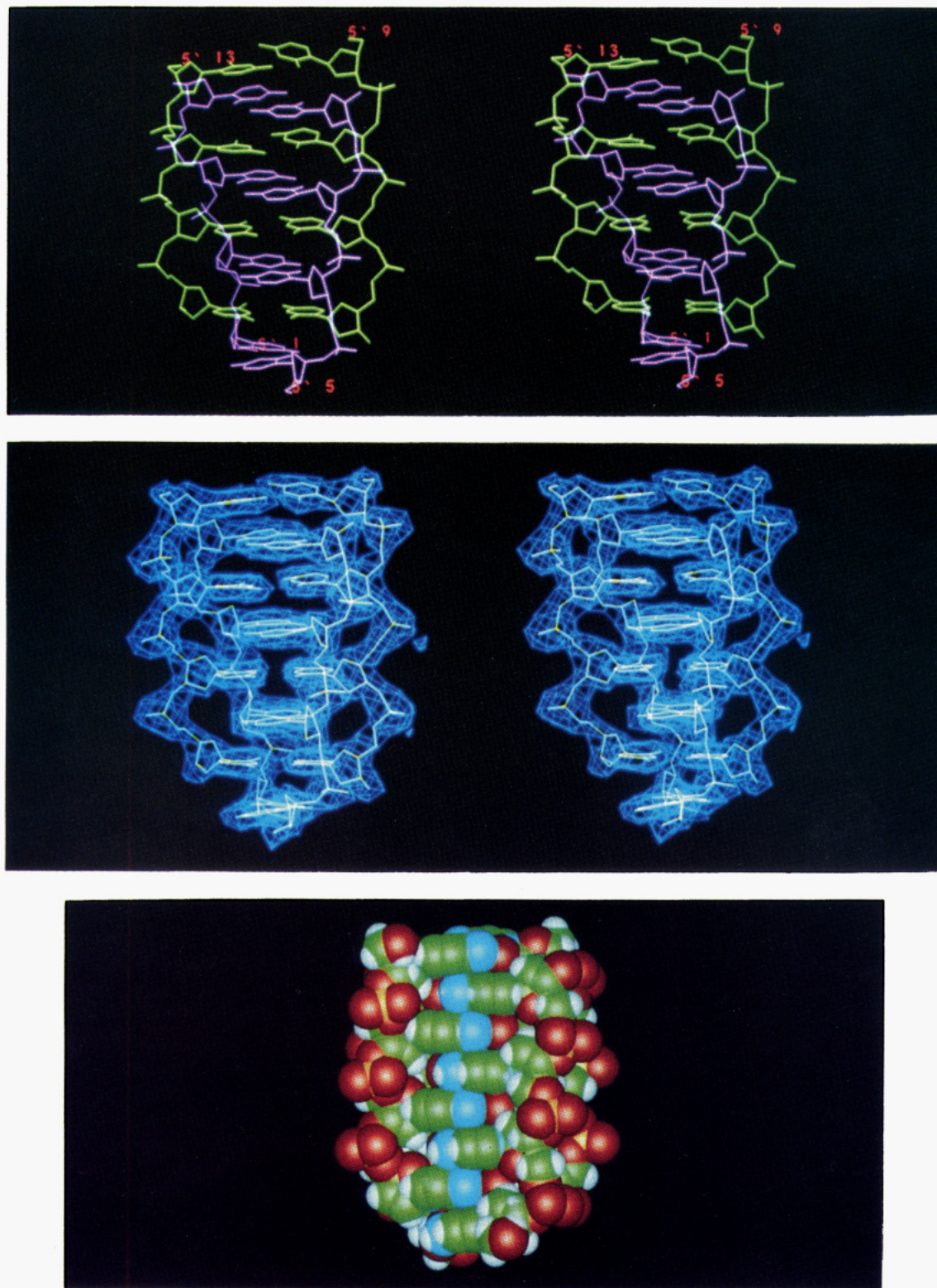


FIGURE 1: Views of the four-stranded molecule A seen largely from the side of the wide groove. (A, top) A stereoscopic skeletal diagram of d(C<sub>4</sub>) is shown. The molecule is made of two parallel paired duplexes which are intercalated into each other. The purple pair has its 5' ends at the bottom of the diagram, while the green pair has its 5' ends at the top. The numbers refer to the nucleotide number at the 5' end of the strand. Strands C1–C4 are parallel to C5–C8. The two green strands are parallel to each other but are oriented in the opposite direction. The molecule is tilted slightly to show the configuration of the hydrogen-bonded C•C<sup>+</sup> base pairs. Careful examination of the figure shows some irregularities in the molecule. Hydrogen atoms are not shown. (B, middle) The molecule is shown in stereo with a blue electron density map ( $2F_o - F_c$ ) contoured at  $1\sigma$ . The map clearly defines the position of sugar, phosphate, and base residues. For clarity, the peaks for water molecules are not shown. (C, bottom) A van der Waals model is shown in which red represents oxygen, yellow is phosphorus, blue is nitrogen, green is carbon, and white is hydrogen.

1993). The sugar residues are dispersed in the two chains in a zigzag array as seen in Figure 3. In each narrow groove there are seven H1'–H1' distances, leading to a total of 28 of these distances in the asymmetric unit. The average

distance of these H1'–H1' separations is  $3.13 \pm 0.37$  Å. This agrees rather well with the distance of 3.0 Å in the NMR nuclear Overhauser effect measurements (Gehring et al., 1993).



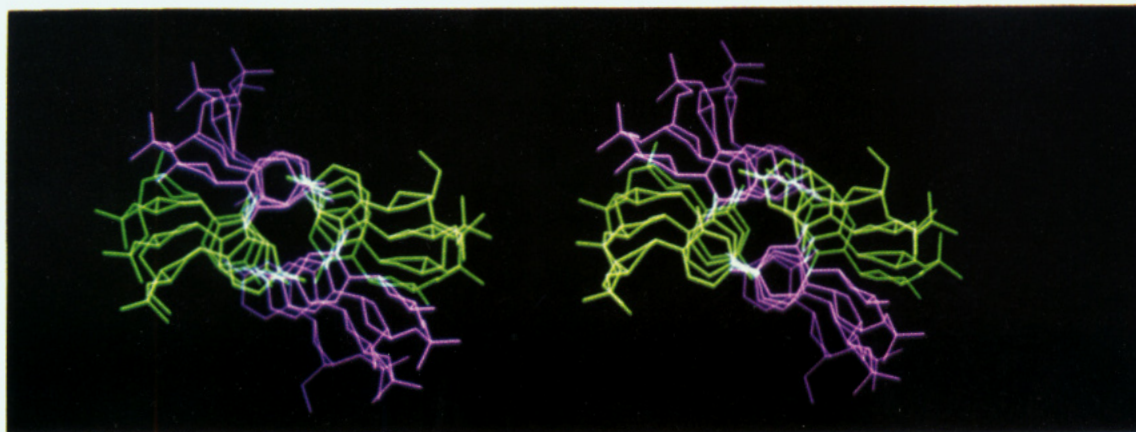


FIGURE 2: A stereoscopic view down the end of molecule A. The strands are colored as in Figure 1A. An empty central region is shown which is filled by hydrogen bonds between the green strands and the purple strands in alternating layers. The slow right-handed helical twist of the ribbon-like array is seen. In the narrow grooves on either side of the molecule, it can be seen that the phosphate groups tend to be tilted away from each other.

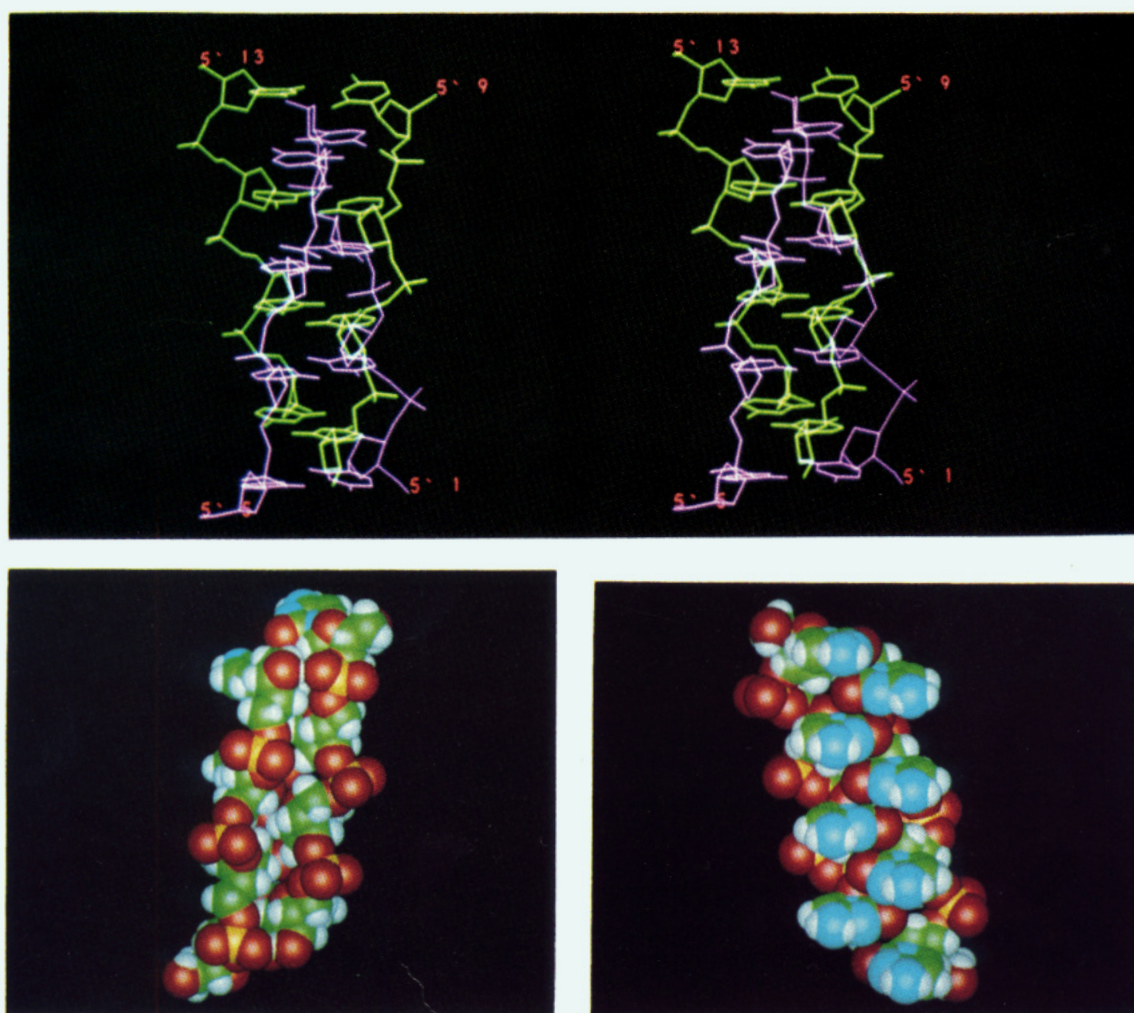


FIGURE 3: Side views. (A, top) A stereoscopic view of the molecule looking into the narrow groove. Molecule A, colored as in Figure 1A, is shown with the two sugar phosphate chains in the foreground. The phosphate groups on one strand occupy a vertical position intermediate between the phosphate positions on the strand in close contact with it. These adjacent strands have opposite polarity. The nucleotide number at the 5' ends of the chains is indicated. Tilting of cytosine 9 relative to the other bases is due to an intermolecular stacking interaction with another molecule. (B, bottom left) A van der Waals diagram showing the two chains closest to the reader in (A). These show the manner in which the antiparallel chains fit into each other intimately, producing some stabilizing van der Waals interactions. (C, bottom right) The two chains furthest away from the viewer in (A) shown in van der Waals representation. The cytosine bases from the two chains are in the foreground of the picture, and the antiparallel chains are behind them. The sugar phosphate chains are slightly more separated in these two strands than in the two strands shown in (B). This difference is also found in molecule B.

**Short Base–Base Stacking.** The detailed manner in which the two duplexes interdigitate is shown in the stereo diagram of Figure 4, which illustrates the relative position of two of

the adjoining base pairs in the structure. The horizontal base pair is 3.1 Å closer to the reader than the vertical base pairs behind it. What is interesting about this view is the fact



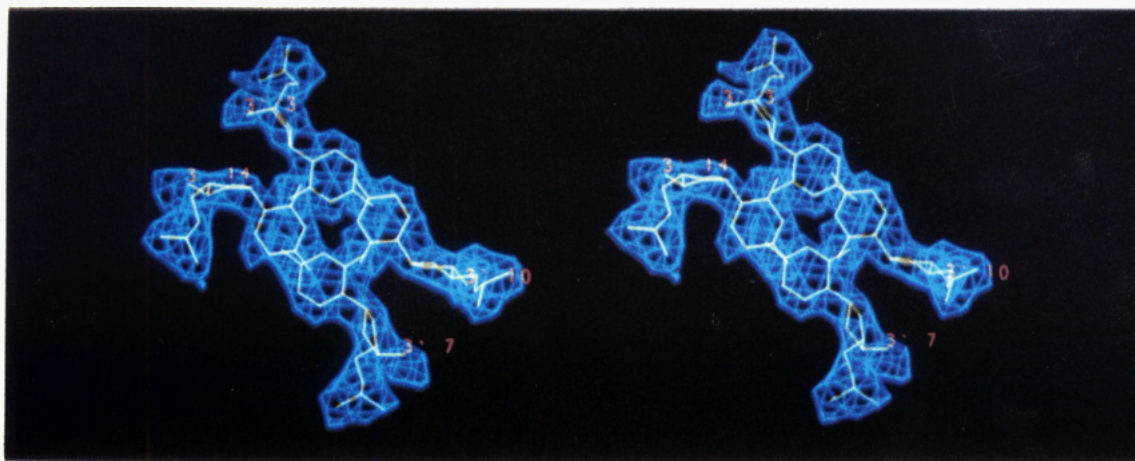


FIGURE 4: A stereo end view of the electron density map surrounding the C-C<sup>+</sup> base pairs involving C14 paired to C10 in the foreground and C3 paired to C7 behind it. It can be seen that the stacking of bases involves only the exocyclic atoms, not the rings themselves. In this packing arrangement, the amino groups in one C-C<sup>+</sup> pair are stacked immediately above the amino groups of the pair below but in the opposite orientation. The same is true for the carbonyl groups as well.

that the intercalation produces a stacking of the bases in which only the exocyclic atoms O2 and N4 are involved in the stacking. The  $\pi$ -electron systems over the rings themselves are not directly involved in stacking. Only the extension of the  $\pi$ -electron system into the exocyclic atoms provides the actual stacking interactions. Base stacking in DNA generally is 3.4 Å, whereas it is observed here at 3.1 Å. This difference in the stacking distance undoubtedly relates to the fact that the interaction only involves the exocyclic components of the  $\pi$ -electron system, rather than the ring itself. Similar stacking distances near 3.1 Å have been seen in small molecule pyrimidine crystals (Green et al., 1962) where only the exocyclic atoms stack on each other but not the rings.

There are three hydrogen bonds that hold the C-C<sup>+</sup> base pair together. The N3–N3 hydrogen bonds in the center of the cytosine pairs have a bond length of  $2.76 \pm 0.08$  Å. The hydrogen bond lengths involving the exocyclic amino group N4 and oxygen O2 have similar lengths of  $2.75 \pm 0.1$  Å. The geometry of the base pairing is thus preserved throughout the 16 base pairs in the asymmetric unit.

The variability in the structure of the molecule is also reflected in differences in the sugar pucker of various residues. There are 32 sugar rings in the asymmetric unit; 15 of them have a C4'-*exo* pucker and five have a C3'-*endo*. Four of the residues have a C2'-*endo* pucker, and since all four are found only at the 5' end of the molecule, it is possible that this pucker may be related to an end effect. There are five C1'-*exo* and three O4'-*endo* puckers. The glycosidic angle  $\chi$  has an average value of 236°. Thus, the ring has a high *anti* conformation.

Molecule A and molecule B are packed laterally with wide groove to wide groove, but there is a tilt close to 30° between their axes. The adjacent pair of molecules interacts using a similar packing motif. The quadruplex molecules thus exist in the form of extended twisted sheets that pack ...ABA'B'... throughout the lattice in which there is slightly more than 30° rotation of the molecular axes between each quadruplex. There is one systematic set of direct hydrogen bonds between molecules A and B. The two phosphate oxygens on C11 receive bifurcated hydrogen bonds from an N4-H on molecule B (distances of 3.04 and 3.27 Å). Many bridging water molecules are found between molecules A and B. In

addition to the lateral interaction through the major groove, there is also a stacking interaction. Molecule A has other molecules stacked on it at both ends. Close inspection of Figure 1A reveals that the cytosine 9 at the 5' end of one strand is tilted somewhat relative to the other bases in the stack. At the bottom the 5' cytosine 5 is also tilted. This tilt is due to the fact that there is a stacking interaction between successive A molecules along the helical axis in which only cytosine 9 from one molecule is stacked upon cytosine 5 of an adjacent molecule. Molecule B, on the other hand, has a stacking interaction only at one end where a crystallographic 2-fold axis is found. At the other end of molecule B, there is no stacking interaction. Instead, the lattice has a cavity there which is near a 3-fold axis. That cavity is large enough to accommodate the platinum atom which goes into it to form the isomorphous derivative used in solving the structure.

At the present stage of refinement 58 water molecules have been identified that are largely found coating the wide groove of the molecule. Water molecules are hydrogen bonded to the hydrogens of amino group N4 which are not involved in the cytosine–cytosine pairing. Other water molecules are also found near phosphate groups. Some of these water molecules are participating in intertetramer interaction; i.e., they are bridging between tetramers A and B, forming hydrogen bonds with the cytosine amino groups and with phosphate oxygens. A full description of this will be published elsewhere.

**Stability of the Quadruplex.** Despite differences in the crystal structure and the NMR structure, what is remarkable is their gross similarity. The X-ray structure reveals much more microheterogeneity than can be visualized in the NMR structure. Differences are found, such as those involving phosphate orientation and the relative positioning of the adjacent chains. On the other hand, there is great similarity in the conclusions regarding the interactions of the bases and the overall packing of the sugar phosphate backbones. Both analyses show a large number of C4'-*exo* puckers. The major difference between them is associated with the helical twist, which is 12.4° between covalently adjacent base pairs in the parallel-stranded duplexes in the X-ray structure versus 16° in the NMR structure. This organization, termed the intercalation motif, is distinctly different from either the DNA



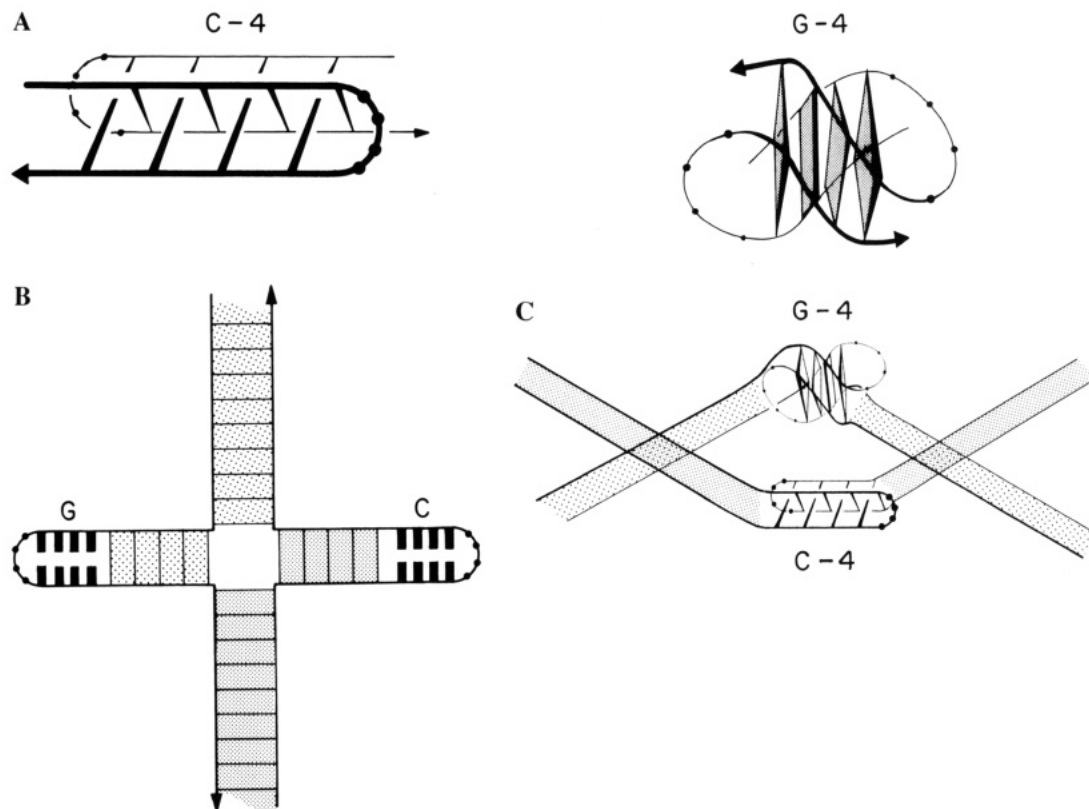


FIGURE 5: Diagrams illustrating the manner in which four-stranded guanine quartet molecules (G-4) and four-stranded cytosine intercalated DNA molecules (C-4) may together stabilize the tips of cruciform extrusions on two identical DNA molecules. (A) Schematic diagram of guanine quartets (G-4) and the cytosine quadruplex (C-4). Shaded squares in G-4 indicate the planar array of four guanine bases. Dots in loops indicate nucleotides. Cross bars in C-4 indicate C-C<sup>+</sup> base pairs between parallel strands. Arrowheads denote the 3' end of the chain. (B) Cruciform extrusion with ends containing C or G bases (short thick bars). Differences in stippling show the way cruciform extrusions stack. (C) Segments of two identical DNA molecules linked by four-stranded G-4 and C-4. The angle between four-way junctions at the core of cruciforms has been shown to be 60° (Murchie et al., 1989). For two identical DNA molecules, there could be a large number of these interactions, leading to cooperativity.

duplexes or the DNA quadruplexes in which four planar guanine residues are found in cyclic hydrogen bonding (Gellert et al., 1962; Kang et al., 1992; Smith & Feigon, 1992). Gehring et al. (1993) have cited several features which may contribute to the stability, including van der Waals stabilization between the sugar phosphate backbones across the narrow groove and the opposite orientation of the carbonyl and amino group dipoles. Another feature which may be stabilizing is the closer stacking of the bases of 3.1 Å, instead of the more familiar 3.4 Å. This base stacking involving only the exocyclic residues may be associated with a larger overlap of the local  $\pi$ -electron clouds which are part of the system of  $\pi$  orbitals around the ring itself. Gehring et al. (1993) have emphasized the fluctuations in the protonation of either one cytosine or the other in the base pairs (Leroy et al., 1993). If these are coordinated, as they suggest, this could lead to further stabilization. Destabilizing features may be associated with the electrostatic repulsion between the phosphate groups in the two chains that are close together. This seems to be minimized by the manner in which the phosphate groups are rotated away from each other so that in some cases significantly larger distances between them are achieved. At the present stage of refinement, we have not been able to assign positions for sodium atoms. It would not be surprising, when further structures of this type are done, to find that these cations reside somewhere in the vicinity of the clustered phosphate groups in the narrow grooves. The differences cited above in the distances between the phosphate groups in the two narrow grooves at

either end of this flat molecule may be associated with an unequal distribution of cations that may be trapped in the crystal lattice.

## DISCUSSION

**Biological Relevance.** It is indeed remarkable that two types of four-stranded molecules have been found in DNA, one involving guanine residues and the other involving cytosine residues. The fact that these two bases are found as complementary pairs in the DNA duplex suggests that such structures may have some biological utility. The interesting feature of these four-stranded molecules is that they both can be assembled in a system in which two loops point in the opposite direction (Kang et al., 1992; Smith & Feigon, 1992). Figure 5A has simple diagrams that show the manner in which both G-4- and C-4-type quadruplexes can form with opposite pointing DNA loops. In the G-4 quadruplex, the guanine residues form with cyclic hydrogen bonding involving four guanines at each level. In the cytosine quadruplex, the chains have the same polarity, but the organization gives rise to hydrogen bonding between two sets of parallel strands involving C-C<sup>+</sup> pairing intercalated between each other.

Sequences containing C-rich and G-rich strands are found in telomeres (Blackburn, 1991) but may also occur in segments scattered throughout the genome. It has been demonstrated that when DNA containing a palindromic sequence of bases is subjected to supercoiling stress, a

cruciform can be extruded in which the palindromic bases on each strand pair together to form the cruciform. If the tips of the cruciform extrusions had segments containing cytosine sequences in one limb and guanine sequences in another (Figure 5B), then two identical molecules of this type could combine together linked by the formation of C-4 and G-4 quadruplexes. This is illustrated in Figure 5C. It has been shown that four-way junctions which form the centers of cruciforms have a configuration such that each of the cruciform extrusions is collinear with segments of the original DNA molecule, but the two segments are arranged at an angle near 60° (Murchie et al., 1989). This means that two cruciform extrusions would be in a position to link together with an identical molecule stabilized by two quadruplexes.

Is it possible that such interactions could be the physical basis whereby identical DNA sequences could bind together? Some suggestions for using quadruplexes in this way have been made (Sen & Gilbert, 1991; Ahmed et al., 1994; Riddlough, 1994). The guanine quadruplex forms at neutral pH; however, the cytosine quadruplex forms only when the pH is lowered. It is possible that such an interaction could be stabilized in a biological system by having specific proteins that bind to the cytosine quadruplex. Guanine quadruplex binding proteins have already been identified (Weisman-Shomer & Fry, 1993; Fang & Cech, 1993; Liu et al., 1993; Schierer & Henderson, 1994). The presence of such proteins stabilizing this interaction could govern whether or not such pairing interactions occur as in meiosis, for example, when identical chromosomes line up with each other. With identical chromosomes many complexes could form and a stabilizing cooperativity would exist. It is unlikely that the cytosine quadruplex would be stabilized at neutral pH in the absence of some stabilizing factor such as a binding protein. Perhaps the presence of such a protein may play an important role in determining the onset of meiosis or other pairing activities. It is clear that further

structural work, as well as molecular biological studies, will be needed to clarify the biological role of systems of this type.

## REFERENCES

- Ahmed, S., Kintanar, A., & Henderson, E. (1994) *Nat. Struct. Biol.* 1, 83.
- Akinrimisi, E. O., Sander, C., & Ts'o, P. O. P. (1963) *Biochemistry* 2, 340.
- Blackburn, E. H. (1991) *Nature* 350, 569.
- Brunger, A. T., Karplus, M., & Petsko, G. A. (1989) *Acta Crystallogr., Sect. A: Found. Crystallogr.* 45, 50.
- Fang, G., & Cech, T. R. (1993) *Cell* 74, 875.
- Gehring, K., Leroy, J.-L., & Guéron, M. (1993) *Nature* 363, 561.
- Gellert, M., Lipsett, M. N., & Davies, D. R. (1962) *Proc. Natl. Acad. Sci. U.S.A.* 48, 2013.
- Green, D. W., Mathews, F. S., & Rich, A. (1962) *J. Biol. Chem.* 237, 3573.
- Hartman, K. A., & Rich, A. (1965) *J. Am. Chem. Soc.* 87, 2033.
- Inman, R. B. (1964) *J. Mol. Biol.* 9, 624.
- Jones, T. A. (1985) *Methods Enzymol.* 115, 157.
- Kang, C. H., Zhang, X., Ratliff, R., Moyzis, R., & Rich, A. (1992) *Nature* 356, 126.
- Langridge, R., & Rich, A. (1963) *Nature* 198, 725.
- Leroy, J.-L., Gehring, K., Kettani, A., & Guéron, M. (1993) *Biochemistry* 32, 6019.
- Liu, Z., Frantz, J. D., Gilbert, W., & Tye, B.-K. (1993) *Proc. Natl. Acad. Sci. U.S.A.* 90, 3157.
- Marsh, R. E., Bierstedt, R., & Eichhorn, E. L. (1962) *Acta Crystallogr.* 15, 310.
- Murchie, A. I. H., Clegg, R. M., von Kitzing, E., Duckett, D. R., Diekmann, S., & Lilley, D. M. J. (1989) *Nature* 341, 763.
- Riddlough, G. (1994) *Nature* 367, 488.
- Schierer, T., & Henderson, E. (1994) *Biochemistry* 33, 2240.
- Sen, D., & Gilbert, W. (1991) *Nature* 344, 364.
- Smith, F. W., & Feigon, J. (1992) *Nature* 356, 164.
- Wang, B. C. (1985) *Methods Enzymol.* 115, 90.
- Weisman-Shomer, P., & Fry, M. (1993) *J. Biol. Chem.* 268, 3306.